ELSEVIER

Thermochimica Acta 398 (2003) 93–99

thermochimica acta

www.elsevier.com/locate/tca

A thermal behaviour study of solid-state cinnamates of the latter trivalent lanthanides and yttrium(III)

M.A.S. Carvalho Filho [a], N.S. Fernandes [b],
F.L. Fertonani [b], M. Ionashiro [b,*]

[a] *Centro Universitário Positivo, UnicenP, Campo Comprido, Curitiba-PR, CEP 81280-330, Brazil*
[b] *Instituto de Química, UNESP, Araraquara-SP, CP 355, CEP 14801-970, Brazil*

Received 25 January 2002; received in revised form 29 April 2002; accepted 8 May 2002

Abstract

Some new compounds of cinnamic acid with the latter trivalent lanthanides and yttrium(III) were synthesized in the solid state. The compounds have the general formula LnL_3, where Ln represents trivalent Eu to Lu or Y ions and L is the cinnamate anion (C_6H_5–CH=CH–COO^-). Thermogravimetry (TG), derivative thermogravimetry (DTG), differential scanning calorimetry (DSC), infrared absorption spectra and X-ray diffraction powder patterns were used to characterize and to study the thermal behaviour of these compounds.

Keywords: Cinnamate; Latter lanthanides and yttrium; Thermal behaviour

---

1. Introduction

Solid-state compounds of cinnamic acid with cobalt(II), nickel(II) and copper(II) metals have been prepared in aqueous solution and characterized by chemical analysis, magnetic moments measurements, vibrational and electronic spectra. Their thermal behaviours were studied by using thermogravimetry and differential thermal analysis [1]. Solid-state compounds of cinnamic acid with manganese(II), zinc(II) and lead(II) metals [2], as well as alkali earth metals, except beryllium and radium [3], have also been prepared from aqueous solutions and they have been studied by using thermoanalytical techniques (TG, DTG, DSC) and X-ray diffraction powder patterns. Thermoanalytical techniques (TG, DTG, DSC), infrared absorption spectra and X-ray diffraction powder patterns were also used to characterize and to study the thermal stability and thermal decomposition of solid-state cinnamates of the former trivalent lanthanides [4].

This paper reports the characterization and thermal analysis studies on the latter trivalent lanthanides and yttrium(III) cinnamates by using X-ray diffraction powder patterns, infrared absorption spectra and thermoanalytical techniques (TG, DTG, DSC).

2. Experimental

The cinnamates of Eu to Lu and Y(III) were prepared by the addition of an aqueous solution of the respective lanthanide or yttrium nitrate to an aqueous solution of sodium cinnamate. The solids obtained were washed with distilled water and ethanol until

---

* Corresponding author.
E-mail address: massaoi@iq.unesp.br (M. Ionashiro).

0040-6031/03/$ – see front matter © 2002 Elsevier Science B.V. All rights reserved.
PII: S0040-6031(02)00325-8

elimination of the nitrate ions and the excess of cinnamate ions, dried in a forced circulation oven at 50 °C and kept in a desiccator over anhydrous calcium chloride. These compounds were studied by TG, DTG, DSC, IR absorption spectroscopy and X-ray diffractometry.

The metal contents of the compounds were determined by complexometric titration with standard 0.01000 M EDTA solution, after samples of the compounds had been ignited to the metal oxide and dissolved in nitric acid solution as such as from the TG curves. The cinnamate contents were determined from the TG curves.

The TG and DTG curves were recorded on a model SDT 2960 thermal analysis system from TA Instruments. The purge gas was an air flow of 150 ml min^{-1}. A heating rate of 20 °C min^{-1} was adopted, with samples weighing about 7 mg. Alumina crucibles were used for recording the TG and DTG curves.

The DSC curves were obtained using a DSC 2010 from TA Instruments. The purge gas was an air flow of 150 ml min^{-1}. A heating rate of 20 °C min^{-1} was adopted, with samples weighing about 5–6 mg and aluminium crucibles with perforated covers.

The X-ray powder patterns were obtained with HGZ 4/B horizontal diffractometer (GDR) equipped with a proportional counter and a pulse height discriminator. The Bragg–Brentano arrangement was adopted, using Co K$_x$ ($\lambda = 1.7889$ Å) and a setting of 38 kV and 20 mA. The infrared spectra were recorded on a Nicolet FTIR-730 spectrophotometer in the spectral range 4000–400 cm^{-1} using KBr pellets.

3. Results and discussion

Table 1 presents the analytical and thermoanalytical (TG) data on the prepared compounds. The chemical analysis results permitted to establish the stoichiometry of the prepared compounds indicating the relation M:L:H_2O = 1:3:0.4 for europium and gadolinium compounds and M:L = 1:3 for the terbium to lutetium and yttrium compounds.

The X-ray powder patterns (Fig. 1) verified that the compounds have a crystalline structure, with evidence of the formation of two isomorphous series. In the first series are the europium to dysprosium compounds. The holmium to lutetium and yttrium compounds belong to the second isomorphous series.

The cinnamate anion has two different potential donor sites for the formation of bonds with metal ions: the carbon–carbon double bond and the oxygen atoms of the carboxyl group. The infrared data were used to elucidate the coordination between the metallic ions and the anionic ligand.

Table 2 lists the main IR bands of the compounds. For the europium and gadolinium cinnamates, the bands in the region 3700–3060 cm^{-1} are assigned to the stretching of the OH group (ν(OH)) from coordinated water. The bands in the region 1634–1636 cm^{-1} are assigned to the ν(c=c) vibrations. It is suggested that the coordination does not take place between the π-electron system of the c=c bond and the metal ions, because a change to lower frequencies, relative to the sodium salt, is not observed in the compounds. However, a significant change to lower frequency

Table 1
Analytical and thermoanalytical (TG) results[a]

Compound	Ligand loss (%)		Metal content (%)			Water (%)	
	Calculated	TG	Calculated	TG	EDTA		
$[EuL_3 \cdot 0.4H_2O]_n$	69.50	69.58	25.30	25.29	25.15	1.20	1.13
$[GdL_3 \cdot 0.4H_2O]_n$	68.90	68.77	25.95	26.03	25.82	1.19	1.23
$[TbL_3]_n$	69.53	69.68	26.47	26.32	26.55	–	–
$[DyL_3]_n$	69.12	68.98	26.90	27.16	27.18	–	–
$[HoL_3]_n$	68.84	68.85	27.20	27.26	27.31	–	–
$[ErL_3]_n$	68.58	68.42	27.47	27.66	27.62	–	–
$[TmL_3]_n$	68.39	68.45	27.67	27.45	27.53	–	–
$[YbL_3]_n$	67.94	67.89	28.16	28.24	28.17	–	–
$[LuL_3]_n$	67.78	67.70	28.33	28.25	28.16	–	–
$[YL_3]_n$	78.71	78.52	16.76	16.99	16.80	–	–

[a] Cinnamate ion.

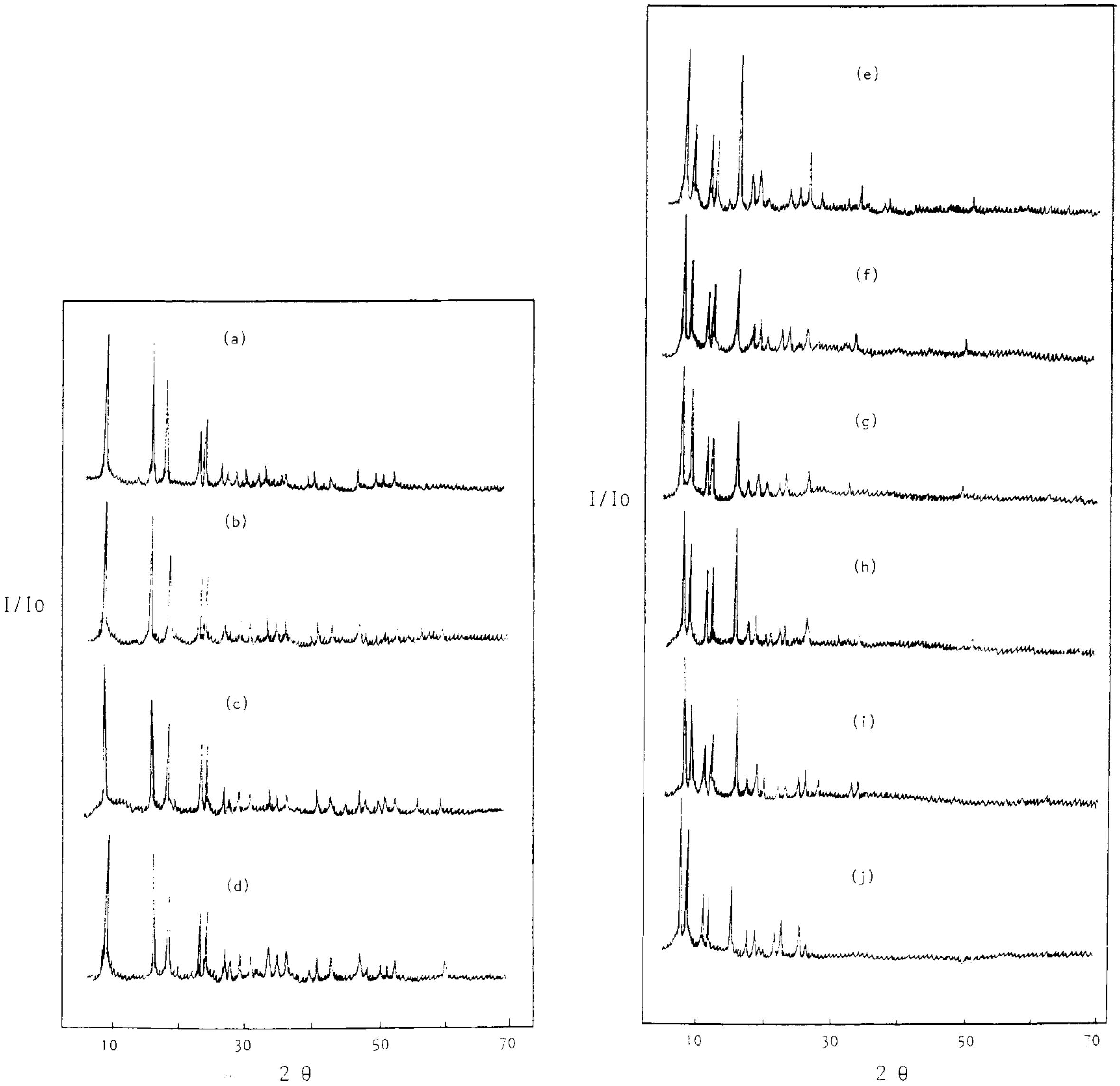

Fig. 1. X-ray powder diffraction patterns of the compounds: (a) $[EuL_3{\cdot}0.4H_2O]_n$; (b) $[GdL_3{\cdot}0.4H_2O]_n$; (c) $[TbL_3]_n$; (d) $[DyL_3]_n$; (e) $[HoL_3]_n$; (f) $[ErL_3]_n$; (g) $[TmL_3]_n$; (h) $[YbL_3]_n$; (i) $[LuL_3]_n$; (j) $[YL_3]_n$ (L = cinnamate).

can be observed for the stretching $\nu(COO^-)$ as compared with that for sodium cinnamate. This confirms that the coordination of the ligand to the metal ions is made through the oxygen atoms of the COO^- groups. The insolubility of the latter lanthanides and yttrium(III) cinnamates in polar and non-polar solvents is in agreement with experimental data found in the literature suggesting a polymeric structure [1,5], and is also in agreement with the experimental data obtained for the former lanthanides cinnamates [4].

TG and DTG curves of the compounds are shown in Fig. 2. For the europium and gadolinium cinnamates, the TG and DTG curves (Fig. 2(a) and (b)) exhibit mass losses in three steps. The first step between 270 and 282 °C is attributed to dehydration, in agreement with the lighter lanthanides cinnamates [4]. The

Table 2
IR spectra (cm^{-1}) of the compounds [$LnL_3\cdot 0.4H_2O$]$_n$ and [LnL_3]$_n$, where Ln represents lanthanides ions and L is the cinnamate ion

Compound	ν(O–H) (H_2O)[a]	ν(COO^-)	ν(C=C)
$NaL\cdot H_2O$	3100–3600	1549 (s)[b]	1637 (s)
[$EuL_3\cdot 0.4H_2O$]$_n$	3060–3700	1503 (s)	1636 (s)
[$GdL_3\cdot 0.4H_2O$]$_n$	3110–3720	1503 (s)	1635 (s)
[TbL_3]$_n$		1503 (s)	1636 (s)
[DyL_3]$_n$		1503 (s)	1636 (s)
[HoL_3]$_n$		1508 (s)	1636 (s)
[ErL_3]$_n$		1508 (s)	1635 (s)
[TmL_3]$_n$		1506 (s)	1634 (s)
[YbL_3]$_n$		1507 (s)	1634 (s)
[LuL_3]$_n$		1507 (s)	1635 (s)
[YL_3]$_n$		1508 (s)	1635 (s)

[a] Stretching frequencies.
[b] Strong.

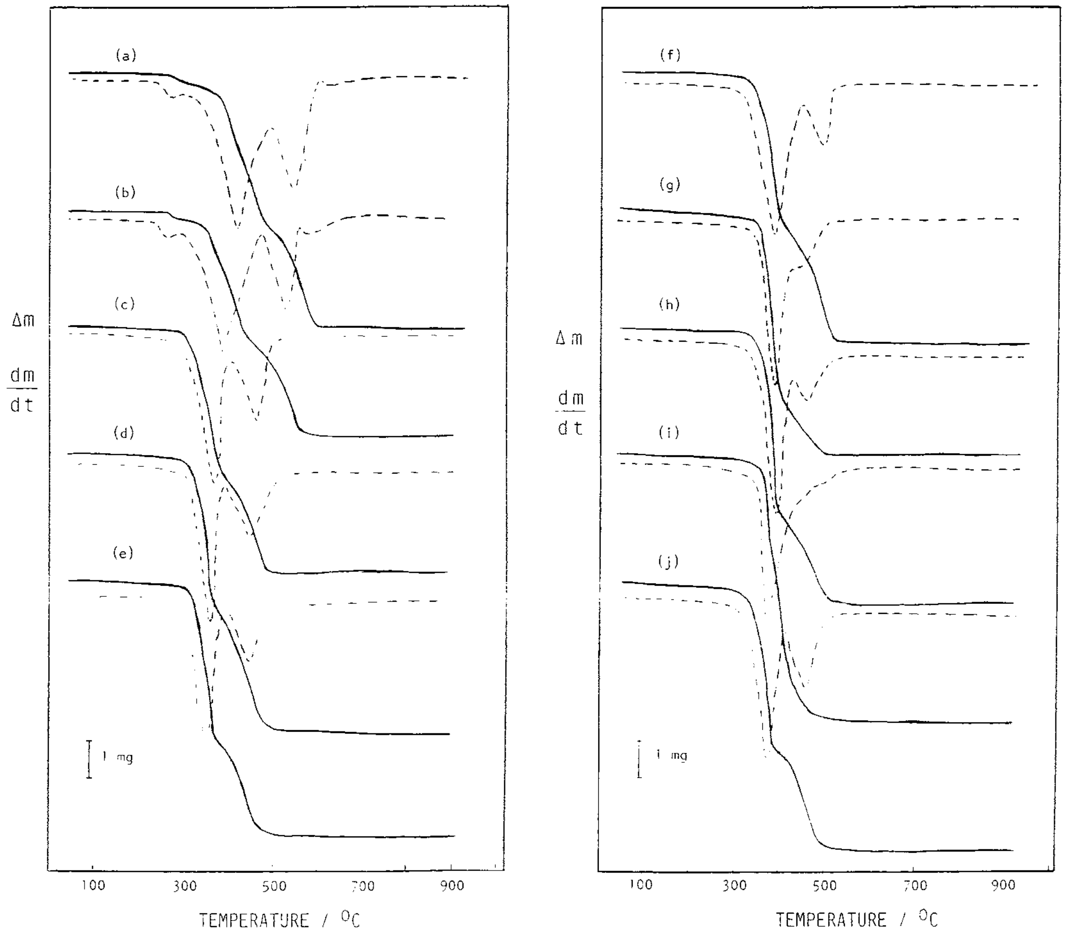

Fig. 2. TG and DTG curves of the compounds: (a) [$EuL_3\cdot 0.4H_2O$]$_n$ (7.327 mg); (b) [$GdL_3\cdot 0.4H_2O$]$_n$ (7.306 mg); (c) [TbL_3]$_n$ (7.391 mg); (d) [DyL_3]$_n$ (8.571 mg); (e) [HoL_3]$_n$ (7.471 mg); (f) [ErL_3]$_n$ (7.391 mg); (g) [TmL_3]$_n$ (8.431 mg); (h) [YbL_3]$_n$ (7.710 mg); (i) [LuL_3]$_n$ (8.087 mg); (j) [YL_3]$_n$ (7.751 mg) (L = cinnamate).

thermal decomposition of the anhydrous compounds occurs in two consecutive steps between 300 and 600 °C (Eu) and 300 and 590 °C (Gd), with the formation of the respective oxides, Eu_2O_3 and Gd_2O_3.

For the terbium to lutetium and yttrium cinnamates, the TG and DTG curves (Fig. 2(c)–(j)) show that these compounds were obtained in the anhydrous form, since no mass loss due to dehydration is observed in the TG curves. The thermal decomposition of the compounds occurs in two consecutive steps between 290 and 550 °C, with formation of the respective oxides, Tb_4O_7 and Ln_2O_3.

The formation of oxy- or dioxycarbonate, $Ln_2O_2CO_3$, as intermediate as reported in the thermal decomposition of lanthanide compounds with 4-dimethylaminobenzylidenepyruvate and 4-methoxybenzylidenepyruvate [6,7] was not observed during the thermal decomposition of the compounds studied in this work.

For the full series of lanthanide(III) cinnamate, the former lanthanides (La–Gd) were obtained as hydrated compounds, while the latter lanthanide (Tb–Lu) cinnamates were obtained in the anhydrous state. For the lighter trivalent lanthanide (La–Sm) cinnamates, except the cerium(III) compound, the dehydration temperature as well as the temperature of thermal decomposition decrease with increasing atomic number of the lanthanide ions. However, for the latter trivalent lanthanides (Eu–Lu) cinnamates, no correlation was found in the temperature of thermal decomposition with the increasing atomic number. The temperature range and the percentage mass loss observed in each step of the thermal decomposition are shown in Table 3.

The DSC curves of the compounds are presented in Fig. 3. These curves show endothermic and exothermic peaks attributed to crystalline transition, fusion and

Table 3
Temperature range and the percentage mass loss observed in each step of the TG curves of the latter lanthanides and yttrium cinnamates[a]

Compound		Steps		
		First	Second	Third
$[EuL_3{\cdot}0.4H_2O]_n$	T (°C)[b]	270–282	300–490	490–600
	Δm (%)[c]	1.13	38.30	31.28
$[GdL_3{\cdot}0.4H_2O]_n$	T (°C)	270–282	300–430	430–590
	Δm (%)	1.23	35.67	33.10
$[TbL_3]_n$	T (°C)	290–390	390–500	
	Δm (%)	41.10	28.58	
$[DyL_3]_n$	T (°C)	290–370	370–510	
	Δm (%)	37.45	31.53	
$[HoL_3]_n$	T (°C)	290–370	370–510	
	Δm (%)	40.40	28.45	
$[ErL_3]_n$	T (°C)	300–400	400–530	
	Δm (%)	36.76	31.66	
$[TmL_3]_n$	T (°C)	310–400	400–520	
	Δm (%)	49.70	18.75	
$[YbL_3]_n$	T (°C)	300–395	395–530	
	Δm (%)	43.30	24.59	
$[LuL_3]_n$	T (°C)	310–400	400–500	
	Δm (%)	38.34	29.26	
$[YL_3]_n$	T (°C)	290–390	390–530	
	Δm (%)	48.05	30.47	

[a] Cinnamate ion.

[b] Temperature.

[c] Mass loss.

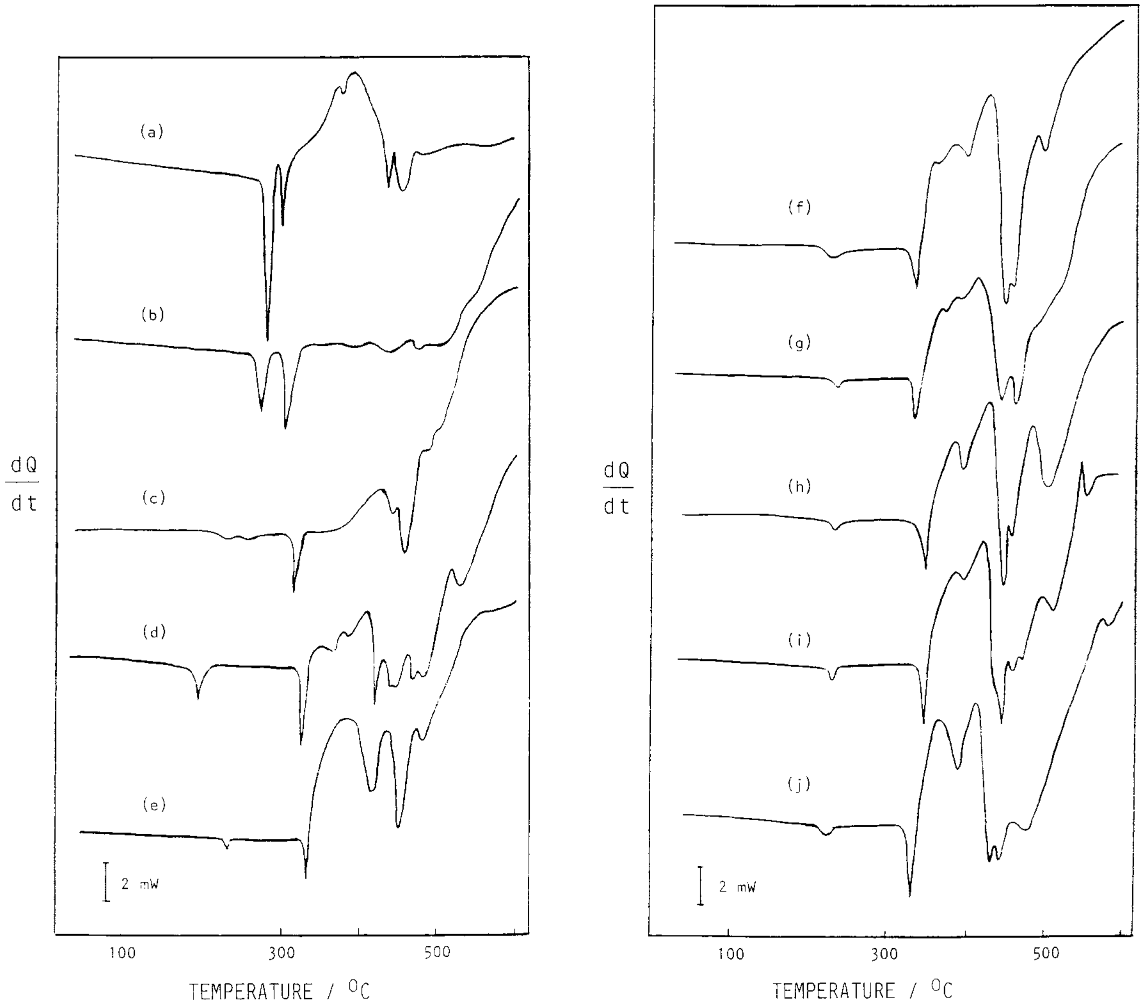

Fig. 3. DSC curves of the compounds: (a) $[EuL_3{\cdot}0.4H_2O]_n$ (5.325 mg); (b) $[GdL_3{\cdot}0.4H_2O]_n$ (5.835 mg); (c) $[TbL_3]_n$ (6.179 mg); (d) $[DyL_3]_n$ (5.431 mg); (e) $[HoL_3]_n$ (5.447 mg); (f) $[ErL_3]_n$ (5.578 mg); (g) $[TmL_3]_n$ (6.089 mg); (h) $[YbL_3]_n$ (6.026 mg); (i) $[LuL_3]_n$ (5.959 mg); (j) $[YL_3]_n$ (6.015 mg) (L = cinnamate).

thermal decomposition. The thermal event attributed to the crystalline transition was confirmed by X-ray diffraction data.

For the europium and gadolinium cinnamates (Fig. 3(a) and (b)), the first endothermic peak at 280 and 275 °C, respectively, is due to the crystalline transition. The second endothermic peak at 300 °C (Eu) and 305 °C (Gd) is attributed to simultaneous fusion and dehydration. The evidence that the dehydration is associated with the fusion was provided by experiments on samples heated in a long glass test tube under approximately the same conditions as those for the DSC curves. In these experiments, simultaneous fusion and water condensation were observed. After the fusion, the DSC curves show a sequence of thermal events in the range 320–480 °C (Eu) and 350–500 °C (Gd) attributed to the oxidation (exo) and thermal decomposition (endothermic) of the organic matter, in correspondence with the first mass loss of the anhydrous compounds observed in the TG curves. The exotherm in the temperature range 520–600 °C (Gd) is attributed to the oxidation of the carbonaceous residue resulting from the anterior step, in correspondence with the last mass loss of the TG curve. For the europium cinnamate, no thermal event is observed in the range 480–600 °C, suggesting that the heat involved in the last mass loss of the TG curve occurs above 600 °C.

For the terbium cinnamate (Fig. 3(c)), the endothermic peaks at 235 and 260 °C are due to the crystalline transition and the endothermic peak at 315 °C is attributed to the fusion of the compound. The exotherm with the peaks at 425 and 450 °C, followed by a endothermic peak at 455 °C are attributed to the oxidation and thermal decomposition of the organic matter, respectively, in correspondence with the first mass loss of TG curve. The exotherm in the temperature range 455–600 °C which beginning overlapped the peak at 455 °C is attributed to the oxidation of the carbonaceous residue resulting from the anterior step, in correspondence with the last mass loss of the TG curve.

For the dysprosium to lutetium and yttrium cinnamates (Fig. 3(d)–(j)), the endothermic peaks at 195 and 325 °C (Dy), 235 and 330 °C (Ho), 230 and 335 °C (Er), 238 and 335 °C (Tm), 235 and 348 °C (Yb), 230 and 345 °C (Lu), 225 and 330 °C (Y) are attributed to the crystalline transition and fusion of the compounds, respectively. In the temperature range that begins immediately after the fusion and up to 500 °C, the exotherm followed by an endotherm, both with two or three peaks, are attributed to the oxidation and thermal decomposition of the organic matter, respectively, in correspondence with the first mass loss of the TG curve. The exotherm in the temperature range 500–600 °C is attributed to the oxidation of the carbonaceous residue resulting from the anterior step, in correspondence with the last mass loss of the TG curve.

4. Conclusion

The TG curves and chemical analyses confirmed a general formula for these solid compounds. The X-ray powder patterns verified that the heavier lanthanides and yttrium cinnamates studied in this work have a crystalline structure, with evidence of formation of two isomorphous series, as well as the crystalline transition that occurs with the heating. The TG, DTG and DTG curves provided previously unreported information concerning the thermal behaviour of these compounds.

Acknowledgements

The authors are grateful to FAPESP (Proc. 85/0853-1 and 97/12853-3) and CNPq for financial support and also to Isilda Marie Aparecida Ogata for the aid in the preparation of the compuscript.

References

[1] J.R. Allan, B.R. Carson, Thermochim. Acta 154 (1989) 315.
[2] M.A.S. Carvalho Filho, M. Ionashiro, Ecl. Quím. 23 (1998) 9.
[3] A.G. Zaina Chiaretto, M.A.S. Carvalho Filho, N.S. Fernandes, M. Ionashiro, Ecl. Quím. 23 (1998) 91.
[4] M.A.S. Carvalho Filho, N.S. Fernandes, M.I.G. Leles, R. Mendes, M. Ionashiro, J. Therm. Anal. Cal. 59 (2000) 669.
[5] J.R. Allan, N.D. Baird, L. Kassyk, J. Therm. Anal. 16 (1979) 79.
[6] M.H. Miyano, C.B. Melios, C.A. Ribeiro, H. Redigolo, M. Ionashiro, Thermochim. Acta 221 (1993) 53.
[7] L.C.S. Oliveira, C.B. Melios, M. Spirandeli Crespi, C.A. Ribeiro, M. Ionashiro, Thermochim. Acta 219 (1993) 215.